

New dry powders for inhalation containing temozolomide-based nanomicelles for improved lung cancer therapy

RÉMI ROSIÈRE¹, MICHEL GELBCKE², VÉRONIQUE MATHIEU³,
PIERRE VAN ANTWERPEN^{2,4}, KARIM AMIGHI¹ and NATHALIE WAUTHOZ¹

¹Laboratory of Pharmaceutics and Biopharmaceutics, ²Laboratory of Therapeutic Chemistry,
³Laboratory of Cancerology and Experimental Toxicology, ⁴Analytical Platform,
Faculty of Pharmacy, Université Libre de Bruxelles (ULB), B-1050 Brussels, Belgium

Received May 6, 2015; Accepted June 22, 2015

DOI: 10.3892/ijo.2015.3092

Abstract. Besides the numerous advantages of a chemotherapy administered by the inhalation route for lung cancer therapy, dry powder for inhalation (DPI) offers many advantages compared to other techniques and seems to be a technique that is well-adapted to an anticancer treatment. DPI formulations were developed using the cytotoxic drug temozolomide and a new folate-grafted self-assembling copolymer, a conjugate

of three components, folate-polyethylene glycol-hydrophobically-modified dextran (F-PEG-HMD). F-PEG-HMD was synthesized using carbodiimide-mediated coupling chemistry in three main steps. F-PEG-HMD was characterized by ¹H-NMR, mass spectrometry and thermal analysis. F-PEG-HMD presented a critical micellar concentration in water of 4×10^{-7} M. F-PEG-HMD nanomicelles were characterized by a trimodal particle size distribution with Z-average diameter of 83 ± 1 nm in water. Temozolomide-loaded nanomicelles were prepared by solubilization of F-PEG-HMD in the presence of temozolomide. Temozolomide solubility in water was increased in the presence of F-PEG-HMD (2-fold increase in molar solubility) which could potentially lead to increased local concentrations in the tumor site. The temozolomide-loaded F-PEG-HMD nanomicelles were characterized by a Z-average diameter of ~ 50 to ~ 60 nm, depending on the F-PEG-HMD concentration used. The nanomicelles were then spray-dried to produce dry powders. Temozolomide remained stable during all the formulation steps, confirmed by similar *in vitro* anticancer properties for the DPI formulations and a raw temozolomide solution. Two of the developed DPI formulations were characterized by good aerodynamic properties (with a fine particle fraction of up to 50%) and were able to release the F-PEG-HMD nanomicelles quickly in aqueous media. Moreover, *in vitro*, the two DPI formulations showed wide pulmonary deposition in the lower respiratory tract where adenocarcinomas are more often found. The present study, therefore, shows that F-PEG-HMD-based dry powders for inhalation could constitute an interesting drug delivery system able to release nanomicelles that are useful in adenocarcinomas that overexpress folate receptors.

Correspondence to: Dr Rémi Rosière, Laboratory of Pharmaceutics and Biopharmaceutics, Faculty of Pharmacy, Université Libre de Bruxelles (ULB), Campus Plaine, CP207, Boulevard du Triomphe, B-1050 Brussels, Belgium
E-mail: rrosiere@ulb.ac.be

Abbreviations: Boc-NH-PEG-NH₂, α -t-Butyloxycarbonylamino- ω -amino poly(ethyleneglycol); CMC, critical micelle concentration; C_{mic}, molar concentration of the micellar F-PEG-HMD; d(0.5), median diameter; DCC, *N,N'*-dicyclohexylcarbodiimide; DCU, *N,N'*-dicyclohexylurea; DLS, dynamic light scattering; DMAP, 4-(dimethylamino)pyridine; DMSO, dimethyl sulfoxide; DPI, dry powder for inhalation; DSC, differential scanning calorimetry; DSS-d₆, 3-(trimethylsilyl)-1-propanesulfonic acid-d₆ sodium salt; EE, entrapment efficiency; ESI, electrospray ion source; (Q-TOF), quadrupole-time of flight; FBS, fetal bovine serum; F, folate; FPF, fine particle fraction; FR, folate receptor; GLC, glucose; GR, graft ratio; HMD, hydrophobically-modified dextran; ¹H NMR, proton nuclear magnetic resonance spectroscopy; IC₅₀, half maximal inhibitory concentrations; MMAD, mass median aerodynamic diameter; MTT, 3-[4,5-dimethylthiazol-2-yl] diphenyltetrazolium bromide; MWCO, molecular weight cut-off; Mw, molecular weight; NHS, *N*-hydroxysuccinimide; PdI, polydispersity index; PEG, polyethylene glycol; RPMI, Roswell Park Memorial Institute medium; NSCLC, non-small cell lung cancers; SLF, simulated lung fluid; ST, stearate; SU, succinate; TEA, triethylamine; TFA, trifluoroacetic acid; TGA, thermogravimetric analysis; TMZ, temozolomide; S_{sat}, TMZ saturation solubility; S_{tot}, total TMZ molar solubility; δ , chemical shifts; *k*, molar solubilization capacity

Key words: lung cancer, non-small cell lung cancer, temozolomide, inhaled chemotherapy, dry powder inhalation, dry powder for inhalation, targeted therapy, self-assembling copolymer, micelle

Introduction

Lung cancer is one of the most frequent types of cancer in the world and remains the most deadly (1). Most lung cancers ($\sim 85\%$) are non-small cell lung cancers (NSCLC), which are mainly represented by adenocarcinomas ($\sim 50\%$) (2). Unlike squamous cell carcinomas ($\sim 20\%$), which are usually located in the bronchi, adenocarcinomas are often found deeper in the lung (2,3). Nowadays, a new updated classification of lung cancers is more appropriate, following the establishment of

a broad global database of cancers (3). Therefore, new histological classifications identifying new targets are provided (2) and allow administration of more personalized treatment to the patient (4). For this purpose, different studies have shown an overexpression of folate receptor (FR), especially FR α , in adenocarcinomas, compared to healthy cells (5-8). In such cases, up to 72% of strongly FR-positive tumors are reported (6).

Conventional or targeted chemotherapies are currently administered through systemic routes. This leads to low, short-term concentration in the tumor site and causes dose-limiting systemic toxicities to the patient. These observations could be partly responsible for the limited 5-year survival rate obtained for lung cancers [18% from 2004 to 2010 in the United States (1)]. Pulmonary delivery could be an interesting alternative for the treatment of lung cancers. Use of this route allows administration of high doses of conventional or targeted chemotherapy directly to the lung tumor site and reduction of systemic distribution and toxicities, significantly enhancing the therapeutic ratio (9). Among approaches for pulmonary delivery, dry powder for inhalation (DPI) offers many advantages for anticancer treatments compared to other techniques (10). DPI-based formulations are in a solid state, which is more stable for long-term storage and better adapted to poorly water-soluble drugs such as conventional cytotoxic chemotherapeutics. Moreover, the DPI devices can deliver high doses and are activated and driven by the patient's inspiratory flow for a short administration time. They are easily transportable and less expensive, require less maintenance and can be manufactured as disposable inhalers to limit device and environmental contamination in comparison with nebulizers. Much development has been done of DPI formulations for lung cancer therapy, confirming the great interest in this approach (10-13).

Nanotechnology applications in medicine, defined as nanomedicine, have led to a number of applications for cancer imaging or treatment (14,15). Nanocarriers or nanovectors consist of a system composed of drugs, polymeric and/or lipid material that improves biokinetics and biodistribution of these drugs and a ligand that increases the specific cancer cell targeting. Using nanocarrier systems presents many advantages in cancer therapy; this is especially true for pulmonary drug delivery in lung cancer therapy. The advantages include the potential to i) increase drug bioavailability (local or systemic), ii) overcome biological barriers (e.g. mucus, membrane), iii) enhance solubility of the drug, iv) avoid or reduce phagocytosis by alveolar macrophages, v) prolong pulmonary residence time, vi) protect drug from degradation, vii) accumulate drug preferentially into tumors, viii) enhance drug internalization by cells and ix) specifically recognize single cancer cells (16-18). Large numbers of studies on designing nanocarriers for tumor targeting that are delivered by the inhalation route have been described (19-22). However, unlike other types of nanocarriers, self-assembling nanomicelles, in particular polymeric self-assembled micelles contained in a DPI formulation, have not been developed so much (23). This is despite their numerous advantages, such as high *in vivo* stability, high potential to increase the water solubility of poorly water-soluble drug, and a high ability to be designed for active targeting (24-26). Self-assembled polymers

are amphiphilic polymers, i.e. they contain both hydrophilic and hydrophobic moieties, and are able to aggregate spontaneously in aqueous media to form nanomicelles (24-26).

In this context, we have developed DPI formulations composed of a new folate-grafted self-assembling copolymer, F-PEG-HMD, derived from a hydrophobically-modified dextran, which is designed to increase the water solubility of poorly-water soluble compounds, such as most cytotoxic agents, by micelle solubilization. We chose the poorly water-soluble drug temozolomide (TMZ) (solubility in water \sim 3 mg/ml). This drug could be a good candidate for the inhalation route in lung cancer therapy and has already been the subject of aerosol development (10,27). TMZ is a prodrug that is activated at physiologic pH to produce a reactive methyl diazotium ion that is able to methylate DNA (28). TMZ induces autophagy (29) followed by late apoptosis (30). Its unique characteristics mean that TMZ is used in the treatment of cancers associated with extremely poor prognoses, such as glioblastomas and melanomas (31). TMZ has also been evaluated in phase II clinical studies for both small cell lung cancer (32) and NSCLC patients (33-35). Moreover, TMZ presents a relatively acceptable safety profile (36), and only rare respiratory adverse reactions have been reported (37).

The aim of the present study was to design and synthesize a new folate-grafted self-assembling copolymer, i.e. F-PEG-HMD, to use it to prepare TMZ-based nanomicelles and to embed the nanomicelles in dry powders for inhalation to allow the nanomicelles to reach the deep lung to combat adenocarcinoma that overexpress FRs.

Materials and methods

Materials. All chemical reagents were of analytical grade and used without further purification. Anhydrous dimethyl sulfoxide (DMSO), *N,N'*-dicyclohexylcarbodiimide (DCC), 4-(dimethylamino)pyridine (DMAP), triethylamine (TEA), deuterium oxide containing 3-(trimethylsilyl)-1-propanesulfonic acid- d_6 sodium salt (DSS- d_6), folic acid, *N*-hydroxysuccinimide (NHS), DMSO- d_6 , trifluoroacetic acid (TFA), 3-[4,5-dimethylthiazol-2-yl] diphenyltetrazolium bromide (MTT), dichloromethane and ethanol were purchased from Sigma-Aldrich (St. Louis, MO, USA). α -*t*-butyloxycarbonylamino- ω -amino poly (ethyl-ene glycol) (Boc-NH-PEG-NH $_2$) was purchased from Iris Biotech GmbH (Marktredwitz, Germany). Stearic acid was purchased from Fagron (Waregem, Belgium). Dextran T10 was purchased from Pharmacosmos (Holbaek, Denmark). Temozolomide (TMZ) was purchased from Shilpa Medicare Ltd (Raichur, India). Roswell Park Memorial Institute medium (RPMI) and folate-free RPMI, fetal bovine serum (FBS), penicillin-streptomycin solution, gentamycin solution and trypsin-EDTA solution were purchased from Life Technologies (Merelbeke, Belgium).

Synthesis of folate-polyethylene glycol-hydrophobically-modified dextran (F-PEG-HMD), and synthesis of hydrophobically-modified dextran-succinate (HMD-succinate). To prepare HMD-succinate, 100 mg of dextran T10 was dissolved in 7 ml of anhydrous DMSO under magnetic stirring. Then 90 mg of stearic acid, 135 mg of DCC and 20 mg of DMAP were added to the DMSO solution and the mixture was

stirred at 60°C for 24 h. To the DMSO solution, 30 mg of succinic anhydride, 80 µl of TEA and 12 mg of DMAP were added and the mixture was stirred at 40°C overnight. The reaction mixture was dialyzed [molecular weight cut-off (MWCO) = 10 kDa, Spectra/Por; Spectrum Labs, Breda, The Netherlands] against ultrapure water and the dialysate was filtrated to remove the byproduct *N,N'*-dicyclohexylurea (DCU) and unreacted DCC and stearic acid. The filtrate was finally lyophilized by means of an Epsilon 1-6 freeze-dryer (Martin Christ GmbH, Osterode am Harz, Germany). The HMD-succinate molecular structure was confirmed by proton nuclear magnetic resonance spectroscopy (¹H NMR) using a Bruker Avance 300 spectrometer (Bruker Biospin SA, Wissembourg, France) in D₂O or in DMSO-*d*₆ at 25°C. ¹H NMR (chemical shifts (δ) are given in ppm relative to DSS-*d*₆) δ(ppm): 0.9 (3H, stearate (ST), CH₃CH₂), 1.3 (28H, ST, CH₃C₁₄H₂₈CH₂) and 1.6 (2H, ST, CH₃CH₂CH₂), 2.5 and 2.7 (4H, succinate (SU), OOCCH₂CH₂COO), 3.3-4.5 (6H, glucose (GLC), C2-6HO), 4.7 (1H, GLC, C1HO), 4.9-5.2 (3H, esterified GLC, C2-4HOCO).

The number of ST chains and of SU groups as a percentage of the total initial hydroxyl group number per HMD-succinate molecule, i.e. the ST-graft ratio (ST-GR) and the SU-graft ratio (SU-GR), respectively, were determined by ¹H NMR using the following equations (1) and (2):

$$(1) \quad \text{ST - GR (\%)} = 100 \times \frac{[(\text{CH}_3)\text{ST}]}{9 \times [(\text{C1HO})\text{GLC}]}$$

$$(2) \quad \text{SU - GR (\%)} = \frac{[(\text{CH}_2\text{CH}_2)\text{SU}] \times \text{ST - GR}}{(4 \times [(\text{CH}_3)\text{ST}]}$$

where [(CH₃)ST] is the integral of the proton peak of ST at 0.9 ppm, [(CH₂CH₂)SU] is the integral of the proton peaks of SU at 2.5 and 2.7 ppm and [(C1HO)GLC] is the integral of the proton peak of GLC monomer peak at 4.7 ppm.

Synthesis of folate-polyethylene glycol (F-PEG). The carboxylic groups of folic acid were first conjugated with the free primary amine of Boc-NH-PEG-NH₂ using an adaptation of previously reported methods (38,39). Briefly, 1.51 g of folic acid was dissolved in 20 ml of anhydrous DMSO containing 420 µl of TEA by sonication. Then 630 mg of DCC, 350 mg of NHS, and 40 mg of DMAP were added to this DMSO solution and the mixture was stirred at room temperature in the dark overnight. The precipitated byproduct, DCU, was filtrated and the filtrate was added to 420 µl of TEA in the presence of 1.1 g of Boc-NH-PEG-NH₂. This solution was stirred in the dark at room temperature for 24 h. The reaction mixture was first dialyzed (MWCO=1 kDa, Spectra/Por; Spectrum Labs) against NaOH 0.1 M in order to eliminate DMSO, ultrafiltrated (MWCO=1 kDa, Ultracel; Merck Millipore, Darmstadt, Germany) against NaOH 0.1 M and then against ultrapure water and finally lyophilized. The F-PEG-NH-Boc molecular structure was confirmed by ¹H NMR in DMSO-*d*₆ at 25°C and folate content value determined by quantitative UV spectrophotometry of the conjugate in methanol using the folic acid extinction coefficient ε value of 28,400 M⁻¹ cm⁻¹ at λ_{max} of 285 nm using an Agilent 8453 UV/Visible Spectrophotometer (Agilent Technologies, Santa Clara, CA, USA). ¹H NMR (DMSO-*d*₆) δ(ppm): 1.4 (9H, Boc, (CH₃)₃COCONH), 3.7

(288H, PEG, CH₂O), 6.9 (2H, folate, benzene), 7.7 (2H, folate, benzene), 8.8 (1H, folate, pteridin). The folate content value was 0.26±0.01 mmol/g (98±5% of the theoretical value, 0.27 mmol/g).

F-PEG-NH-Boc was then dissolved in 4 ml of dichloromethane under magnetic stirring. To this, 4 ml of TFA were added and the mixture was left to stir overnight. Dichloromethane was evaporated under vacuum and the resulting TFA solution was carefully added dropwise directly into a beaker containing 4.5 g of NaHCO₃ and 5 g of ice. Neutralization occurred until the end of the production of gas bubbles corresponding to CO₂ formation. The reaction mixture was ultrafiltrated (MWCO = 1 kDa) against ultrapure water and lyophilized. The deprotection of the primary amine to form F-PEG-NH₂ was evaluated by ¹H NMR in DMSO-*d*₆ at 25°C and was 100% efficient.

Synthesis of F-PEG-HMD. To synthesize F-PEG-HMD, 45 mg of HMD-succinate was dissolved in the presence of 210 mg of Folate-PEG-NH₂ in 10 ml of anhydrous DMSO under magnetic stirring. Then 25 mg of DCC, 15 mg of NHS, 16 µl of TEA and 5 mg of DMAP were added to this solution and the mixture was stirred at 40°C for 24 h. The reaction mixture was dialyzed (MWCO = 10 kDa) against ultrapure water in order to remove DMSO, then ultrafiltrated (MWCO = 10 kDa) against a 70% (v/v) ethanol solution. Ethanol was evaporated under vacuum and the resulting aqueous solution was lyophilized. The F-PEG-HMD molecular structure was confirmed by ¹H NMR in D₂O at 25°C. ¹H-NMR (D₂O) δ(ppm): 0.9 (3H, ST, CH₃CH₂), 1.3 (28H, ST, CH₃C₁₄H₂₈CH₂) and 1.6 (2H, ST, CH₃CH₂CH₂), 2.5 and 2.7 (4H, SU, OOCCH₂CH₂COO), 3.3-4.5 (6H, GLC, C2-6HO), 3.7 (288H, PEG, CH₂O), 4.9-5.2 (3H, esterified GLC, C2-4HOCO), 6.9 (2H, folate, benzene), 7.7 (2H, folate, benzene), 8.8 (1H, folate, pteridin).

Characterization of F-PEG-HMD

Determination of the PEG-graft ratio. The graft ratio of PEG on HMD as a percentage of the total initial hydroxyl group number per HMD molecule (PEG-GR) was determined by ¹H NMR in D₂O at 25°C using the following equation (3):

$$(3) \quad \text{PEG - GR (\%)} = \frac{4 \times [\text{PEG}] \times [\text{SU - GR}]}{(3 \times n \text{ H}^+ \text{ PEG} \times [(\text{CH}_2\text{CH}_2)\text{SU}]}$$

where [PEG] is the integral of the proton peak of PEG at 3.7 ppm (CH₂O); [SU-GR%] is the SU-Graft ratio (%) of HMD-COOH, n H⁺ PEG is the number of protons per PEG chain according to the molecular weight (Mw) of PEG given by the supplier (Mw=3317, n H⁺ PEG=288) and [(CH₂CH₂)SU] is the integral of the proton peaks of SU at 2.5 and 2.7 ppm.

Determination of the molecular weight range. The Mw range of F-PEG-HMD was determined by direct infusion in a 6520 series electrospray ion source (ESI)-quadrupole-time of flight (Q-TOF) mass spectrometer (Agilent Technologies). The acquisition mode was positive and the Mw was obtained after deconvolution of the mass spectra.

Thermal properties-thermogravimetric analysis and differential scanning calorimetry. The degradation temperature of F-PEG-HMD was determined by thermogravimetric analysis

Table I. Composition and physicochemical properties of the nanomicelle solutions.

Formulations	Composition		Physicochemical properties		
	F-PEG-HMD (mg/ml)	Temozolomide (mg/ml)	Z-average (nm)	PdI ^a	EE ^d (% w/w)
F-PEG-HMD	1	/	83±1 ^b	0.46±0.01 ^b	/
Empty NS-1	1	/	56.8±0.4 ^c	0.43±0.03 ^c	/
Empty NS-9	9	/	68±1 ^c	0.43±0.04 ^c	/
NS-1	1	3.6	50±1 ^c	0.38±0.02 ^c	6±3
NS-3	3	4.0	53±1 ^c	0.37±0.01 ^c	9±2
NS-5	5	4.8	60±4 ^c	0.38±0.02 ^c	9.5±0.7
NS-9	9	4.9	61±3 ^c	0.44±0.07 ^c	8.9±0.8

^aPolydispersity index. ^bDetermined in ultrapure water at 25°C. ^cDetermined in a phosphate buffer at pH 5.0 at 25°C. ^dEntrapment efficiency. ^{b-d}Results are expressed as mean ± SD (n=3).

(TGA) using a Q500 apparatus (TA Instruments, Zellik, Belgium) and Universal Analysis 2000 version 4.4A software (TA Instruments). The run on ~5 mg of F-PEG-HMD was set from 25 to 300°C at a heating rate of 10°C/min.

The thermal properties of F-PEG-HMD were determined by differential scanning calorimetry (DSC) using a Q2000 differential scanning calorimeter coupled to a refrigerated cooling system (TA Instruments). Results were analyzed using Universal Analysis 2000 version 4.4A software (TA Instruments). Approximately 10 mg of F-PEG-HMD were placed in a Tzero hermetic aluminium pan. The heat run was set from 0 to 190°C at 20°C/min using nitrogen as the blanket gas.

Determination of the critical micellar concentration, and the size and zeta potential of the nanomicelles in water. The critical micellar concentration (CMC), defined as the concentration at which F-PEG-HMD starts to self-assemble and aggregate as a nanomicelle, was determined by dynamic light scattering (DLS) in ultrapure water at 25°C using a Malvern Zetasizer nano ZS (Malvern Instruments, Worcestershire, UK) according to the manufacturer's instructions. Briefly, F-PEG-HMD solutions were prepared at concentration of 1-10⁻⁴ mg/ml in ultrapure water at room temperature. The intensity of scattered light was measured in triplicate and plotted for each solution. The CMC corresponds to the concentration at which the intensity of scattered light measured increases due to the presence of nanomicelles.

The particle size distribution, the Z-average mean diameter (Z-average) and the polydispersity index (PdI) of the nanomicelles were determined at a concentration of 1 mg/ml F-PEG-HMD in ultrapure water by DLS. The zeta potential was determined by laser Doppler electrophoresis in ultrapure water using the same apparatus as for size measurement. Each parameter was measured in triplicate and the results are expressed as mean ± SD.

Preformulation investigation - micellar solubilization of TMZ. TMZ saturation solubility in the absence (S_{sat}) or presence of F-PEG-HMD (1, 5, 10, 15 and 20 mg/ml, corresponding to mean molar concentrations of 0.023, 0.116, 0.232, 0.349 and

0.465 mM, respectively) was determined in a phosphate buffer (20.14 mM) at pH 5.0 (European Pharmacopeia 7.0). Briefly, 1 ml buffer containing F-PEG-HMD and ~7 mg TMZ was prepared and left to dissolve at 50°C in an ultrasonic bath until complete dissolution. The solutions were then placed under mild rotating stirring overnight at room temperature and then centrifuged at 3,000 x g at room temperature using a Heraeus Multifuge X1R centrifuge (Thermo Fisher Scientific, Waltham, MA, USA). The supernatants were then collected and analyzed in terms of TMZ content using the validated HPLC method described by Wauthoz *et al.* (10,27). The total TMZ molar solubility (S_{tot}) values were plotted for each molar concentration of the micellar F-PEG-HMD [C_{mic}, which corresponds to the concentration of F-PEG-HMD, as CMC is negligible regarding concentrations of F-PEG-HMD (40)]. The slope of the curve corresponds to the molar solubilization capacity (*k*) value, defined as the number of moles of TMZ that can be solubilized by 1 mol of micellar F-PEG-HMD (40). Each supernatant was analyzed in triplicate and the results are expressed as mean ± SD.

Preparation of dry powders. All manipulation procedures concerning protection of the manipulator and the environment have been previously described by Wauthoz *et al.* (10).

F-PEG-HMD nanomicelle solutions were first prepared by solubilization of F-PEG-HMD in the absence (Empty NS-1 and Empty NS-9) or presence of TMZ (NS-1, NS-3, NS-5 and NS-9) as described in Table I. Briefly, F-PEG-HMD was dissolved with or without TMZ in a phosphate buffer at pH 5.0 (European Pharmacopeia 7.0) at 50°C using an ultrasonic bath. The resulting solutions were cooled at room temperature and then analyzed in terms of size (particle size distribution, Z-average and PdI) and entrapment efficiency (EE). The composition and physicochemical properties of Empty NS-1, Empty NS-9, NS-1, NS-3, NS-5 and NS-9 micellar solutions are presented in Table I. EE is defined as the mass proportion of TMZ entrapped by nanomicelles relative to total TMZ and determined using the following equation (4):

$$(4) \quad EE (\%) = 100 \times \frac{C_{\text{total TMZ}} - C_{\text{non micellar TMZ}}}{C_{\text{total TMZ}}}$$

Table II. Theoretical compositions and actual temozolomide content of SD-2.5, SD-7.5, SD-12.5 and SD-22.5 formulations after spray-drying.

Formulations	Composition of the dry powder formulations [% (w/w)]				Actual TMZ content ^b
	Theoretical composition after spray drying				
	F-PEG-HMD	Leucine	Mannitol	TMZ ^a	
SD-2.5	2.5	20	68.5	9	8.4±0.2
SD-7.5	7.5	20	62.5	10	10.23±0.04
SD-12.5	12.5	20	55.5	19.2	12.2±0.4
SD-22.5	22.5	20	72.4	19.6	11.9±0.2

^aTemozolomide. ^bResults are expressed as mean ± SD contents (n=3).

where $C_{\text{total TMZ}}$ is the total TMZ mass concentration and $C_{\text{non micellar TMZ}}$ is the TMZ mass concentration determined after centrifugal ultrafiltration (Microsep 1 kDa; Pall Life Sciences, Hoegaarden, Belgium). All TMZ contents were determined using the validated HPLC method described elsewhere (10,27). Solutions were prepared three times. Results are expressed as mean ± SD.

The NS-1, NS-3, NS-5 and NS-9 micellar solutions were then spray-dried in the presence of leucine and mannitol (SD-2.5, SD-7.5, SD-12.5 and SD-22.5 formulations, respectively) using a Mini Spray Dryer B-290 (Büchi Laboratory-Techniques, Flawil, Switzerland) under the following conditions: spraying air flow 800 l/h; drying air flow 35 m³/h; solution feed rate 4.4 g/min; nozzle diameter 0.7 mm; inlet temperature 160°C, corresponding to an outlet temperature of ~69°C. The powders were blown through a high performance cyclone, collected in a container and stored in a desiccator at room temperature. Actual TMZ contents of the formulations were determined using the HPLC method. Results are expressed as mean ± SD (n=3). Theoretical compositions of SD-2.5, SD-7.5, SD-12.5 and SD-22.5 formulations after spray-drying and actual TMZ content are presented in Table II.

The ability of the SD-2.5, SD-7.5, SD-12.5 and SD-22.5 formulations to release the F-PEG-HMD nanomicelles in aqueous media was evaluated. Briefly, ~10 mg of dry powder was left to dissolve in 1.5 ml pH 5.0 phosphate buffer for 30 min under gentle rotational agitation. It was then vortexed using an L46 vortex (Labinco B.V., Breda, The Netherlands) twice for 60 sec and finally centrifuged (2,000 x g for 10 min). Particle size distribution of the supernatants was determined in triplicate.

Aerodynamic performance of the dry powders. Dry powders were characterized in terms of their *in vitro* pulmonary deposition, mass median aerodynamic diameter (MMAD) and fine particle fraction (FPF) by performing impaction tests as described for TMZ-based dry powders by Wauthoz *et al* (10). Briefly, the dry powder inhaler was an Axahaler[®] (SMB Laboratories, Brussels, Belgium) loaded with a N³ HPMC capsule containing ~20 mg dry powder for each test. A multi-stage liquid impinger (Copley Scientific, Nottingham, UK) (Apparatus C in the European Pharmacopeia 7.0) was used at a flow rate of 100 l/min for 2.4 sec. The contents of each stage

were collected using a 0.5% v/w acetic acid solution. TMZ contents were then determined using the HPLC method. The FPF is the dose of fine particles (i.e. presenting an aerodynamic diameter ≤5 μm) and is expressed as a percentage of the total dose recovered through the impinger. Each dry powder formulation was evaluated in triplicate and the results are expressed as mean ± SD.

***In vitro* release kinetics of temozolomide.** The *in vitro* release kinetics of TMZ from the SD-2.5 and SD-7.5 dry powder formulations were determined in simulated lung fluid (SLF) (41), at pH 5.0 to guarantee the stability of TMZ, by an adapted dialysis method (42). The TMZ release from raw TMZ (median diameter of particle distribution (d(0.5)) = 21.3±0.4 μm) in the same conditions was used as a control for the method. Briefly, an amount of dry powder formulation corresponding to ~4 mg of TMZ was dispersed in 2 ml of SLF and placed in a dialysis membrane (MWCO = 10 kDa), then placed in 800 ml of SLF maintained at 37±1°C under magnetic agitation (200 rpm). The percentages of dissolved TMZ were determined by the HPLC method at different times up to 160 min. The 100% TMZ dissolution concentration corresponds to the TMZ concentration at 160 min (n=3).

Cell culture. Murine M109-HiFR lung carcinoma cell subline (43) was kindly provided by Dr Hilary Shmeeda from Shaare Zedek Medical Center (Jerusalem, Israel). It was cultured in folate-free RPMI supplemented with 10% FBS, 1% penicillin-streptomycin and 0.02% gentamycin in atmosphere containing 5% CO₂ at 37°C. Human A549 NSCLC cell line (from the American Type Culture Collection, Manassas, VA, USA; code CCL-185) was cultured in RPMI in the same conditions.

***In vitro* anti-proliferative properties of the dry powders.** The anti-proliferative properties of the dry powders were determined by means of a colorimetric MTT assay (27,44,45) using two lung cancer cell lines (M109-HiFR and A549 cell lines). Briefly, cells were allowed to grow in a 96-well plate with a flat bottom with 20,000 or 1,100 cells/well of M109-HiFR or the A549 cell line, respectively. After a 24-h period of incubation at 37°C, the culture medium was replaced by folate-free RPMI containing a raw TMZ solution (positive control), formulation

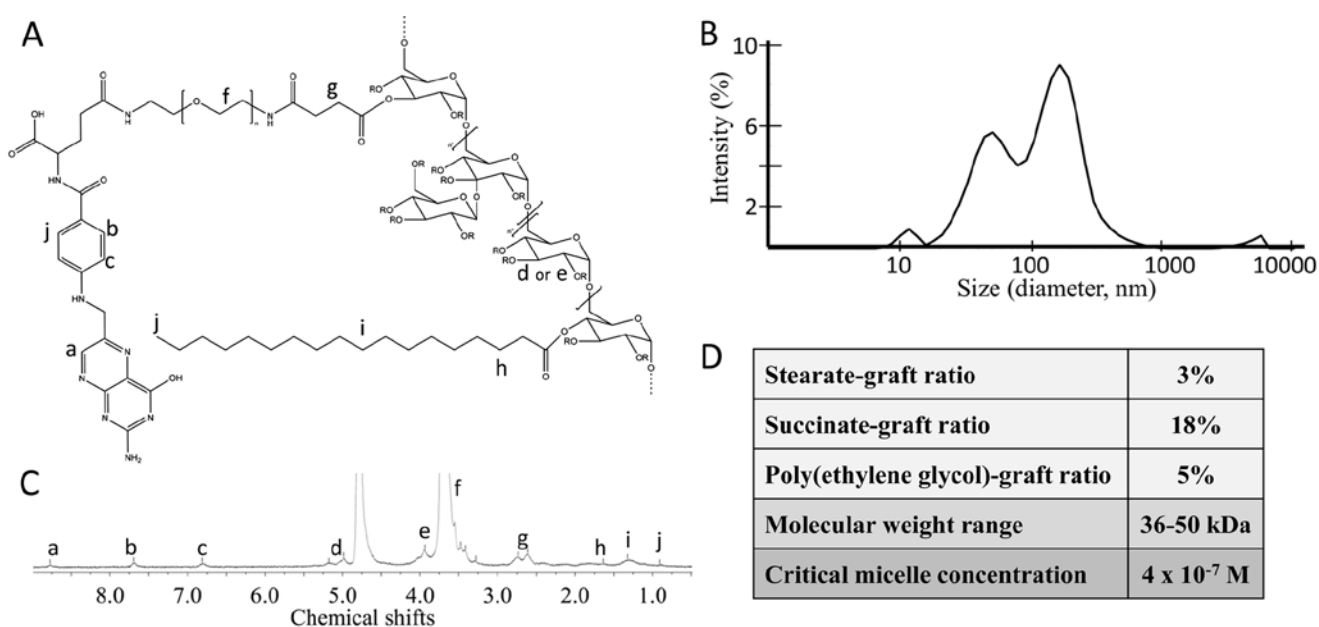


Figure 1. Chemical structure and physicochemical characteristics of F-PEG-HMD. (A) Chemical structure (R group corresponds to -H or succinate or stearate or F-PEG-succinate). (B) Particle size distribution of the F-PEG-HMD nanomicelles in water. (C) ^1H NMR spectra in D_2O . (D) Physicochemical characteristics.

SD-2.5, formulation SD-7.5 or formulation SD-7.5 without TMZ (TMZ-free SD-7.5). The cells were incubated for 2 h with formulations and left to grow for 72 h in the appropriate supplemented medium. The TMZ-relative concentrations that were tested were 10^{-6} M, 5.10^{-6} M, 10^{-5} M, 5.10^{-5} M, 10^{-4} M, 5.10^{-4} M, 10^{-3} M, 5.10^{-3} M and 10^{-2} M. The test measures the number of metabolically active living cells that are able to reduce the yellow MTT to blue formazan by mitochondrial reduction. The amount of formazan obtained is directly proportionate to the number of living cells. It was measured by spectrophotometry using a Bio-Rad 680XR spectrometer (Bio-Rad Laboratories, Nazareth, Belgium) at 570 nm (with a reference of 630 nm). The half maximal inhibitory concentrations (IC_{50} values relative to TMZ) were defined as the TMZ concentrations that inhibit 50% of cells from growing, compared to the untreated control. The experiment was carried out once, in six replicates. Results are expressed as the mean \pm SEM.

Results

Synthesis and characterization of F-PEG-HMD.

F-PEG-HMD was successfully synthesized in three main steps using carbodiimide-mediated coupling chemistry: i) synthesis of HMD-succinate, ii) synthesis of F-PEG and iii) grafting of F-PEG on HMD-succinate. Carbodiimide derivatives, assisted by NHS and DMAP, allowed the formation of both amide linkage (i.e. synthesis of F-PEG) and ester linkage (i.e. synthesis of HMD-succinate and F-PEG-HMD). This carbodiimide-mediated coupling method was effective in both DMSO and water using DCC and EDC, respectively. The chemical structure of each intermediate (i.e. HMD-succinate and F-PEG) was determined using ^1H NMR after purification by ultrafiltration. Folate content was determined in F-PEG using UV spectroscopy. The folate content value in F-PEG was 0.26 ± 0.01 mmol/g ($98 \pm 5\%$ of the theoretical value, 0.27 mmol/g).

The chemical structure of F-PEG-HMD is presented in Fig. 1A. F-PEG-HMD consists of an amphiphilic copolymer formed by a hydrophobic moiety, the grafted stearate chains and a hydrophilic moiety, the dextran polymer on which PEG chains are grafted. Once in the presence of aqueous media, F-PEG-HMD self-assembled as nanomicelles with a hydrophobic core composed of the stearate chains, a hydrophilic corona composed of dextran and PEG chains and folate moieties at the extremities of most of the PEG chains.

^1H NMR confirmed the successful synthesis and the chemical structure of F-PEG-HMD, with characteristic peaks at 0.9, 1.3 and 1.6 ppm for stearate chains, between 3.3 and 4.5 ppm for dextran polymer, at 3.7 ppm for PEG chains and at 6.9, 7.7 and 8.8 ppm for folate groups (Fig. 1C). Grafting of stearate and succinate groups on dextran chains was also confirmed by proton peaks between 4.9 and 5.2 ppm (i.e. using DMSO-d_6 as solvent). These peaks correspond to protons of esterified glucose monomers (i.e. the three protons on C2, C3 and C4). Residual non-esterified glucose monomers have characteristic peaks between 3.3 and 4.5 ppm. F-PEG-HMD is characterized by an ST-GR, SU-GR and PEG-GR of 3, 18 and 5%, respectively (Fig. 1D). Mass spectrometry also confirmed engraftment of the different parts of the copolymer F-PEG-HMD; the Mw range observed was from 36 to 50 kDa (Fig. 1D).

CMC (in a defined solvent) is an important characteristic of self-assembled copolymers because it relates to the stability of the micelles formed in a medium (24-26,46). Below this CMC, the copolymer will be present in the solvent as a solubilized single copolymer chain. However, once the CMC is reached, the copolymer chains will start to aggregate and self-assemble to form micelles, a structure that is thermodynamically more stable at this concentration. It is evident that below the CMC (i.e. after dilution of the copolymer in large physiologic media), the drug contained in the micelles will be released in the bulk medium. The CMC of F-PEG-HMD was determined in ultrapure water at 25°C by DLS; the CMC

observed was 0.02 mg/ml or 4×10^{-7} M. This CMC is lower than that of most surfactants and is slightly lower than that of most lipopolymer conjugates, which are usually characterized by a CMC of up to 10^{-6} M (25), suggesting a good stability of the F-PEG-HMD-formed nanomicelles. In water at 25°C, the nanomicelles are characterized by a trimodal particle size distribution, with maximum particle diameter peaks at ~180, ~50 and ~10 nm, represented by a relative intensity of ~61, ~36 and ~2%, respectively (Fig. 1B). The Z-average and PdI observed was 83 ± 1 nm and 0.46 ± 0.01 (Table I), respectively. Such a polydispersed particle size distribution is possibly due to non-homogeneous grafting over the dextran backbone, a characteristic that is usually observed in grafted copolymers (26). The PEG and stearate chains are grafted randomly throughout the dextran chain; therefore, different aggregations can occur as well as different aggregation numbers (i.e. the number of copolymer chains involved in forming a micelle), resulting in different particle sizes. For example, in a certain conformation, hydrophobic stearate chains may be positioned close to the water, leading to a large particle size. In addition, depending on the stearate grafting, one copolymer chain may form a micelle itself, i.e. a micelle with an aggregation number of 1, resulting in a small particle size (26). The zeta potential observed was -16.8 ± 0.2 mV.

Thermal analysis showed a thermal degradation of F-PEG-HMD characterized by a consequent loss of weight starting from ~150°C (loss of weight of 3% up to 200°C). DSC analysis showed an endothermic peak at 50°C, which corresponds to the melting of PEG and stearate chains (references given by the suppliers). It also showed a glass transition (T_g midpoint) at ~117°C, which was believed to correspond to the T_g of the dextran part (47).

Preformulation investigation - micellar solubilization of TMZ.

In order to observe the ability of F-PEG-HMD nanomicelles to increase TMZ's solubility in aqueous media, TMZ saturation solubility was determined in the absence or presence of 1, 5, 10, 15 and 20 mg/ml F-PEG-HMD (corresponding to mean molar concentrations of 0.023, 0.116, 0.232, 0.349 and 0.465 mM, respectively) in a phosphate buffer at room temperature. A phosphate buffer at pH 5.0 was used to guarantee the stability of TMZ. In addition to making a first approximate estimate of TMZ saturation solubility in physiologic media, the present study was carried out to produce dry powders with the highest TMZ loading from an initial TMZ/F-PEG-HMD solution. Fig. 2 shows the S_{tot} observed for each tested C_{mic} . With regard to the data, F-PEG-HMD nanomicelles increase TMZ solubility in aqueous media to a maximum of a 2-fold increase in TMZ saturation solubility (~15 and ~30 mM in the absence or presence of 20 mg/ml F-PEG-HMD, respectively). This solubility increase appeared to be non-linear (Fig. 2) in the range of tested F-PEG-HMD concentrations. This result suggests a modification of the structure and/or aggregation of the nanomicelles. Two regression lines were drawn: the first for C_{mic} up to ~0.11 mM ($R^2=0.98$) and the second for C_{mic} from ~0.11 to ~0.45 mM ($R^2=0.94$), leading to two molar solubilization capacity values ($k_1=79.56$ and $k_2=11.26$). The results indicate that for low F-PEG-HMD concentrations (less than ~0.11 mM), the capacity of the copolymer to solubilize is higher than for high concentrations (more than ~0.11 mM).

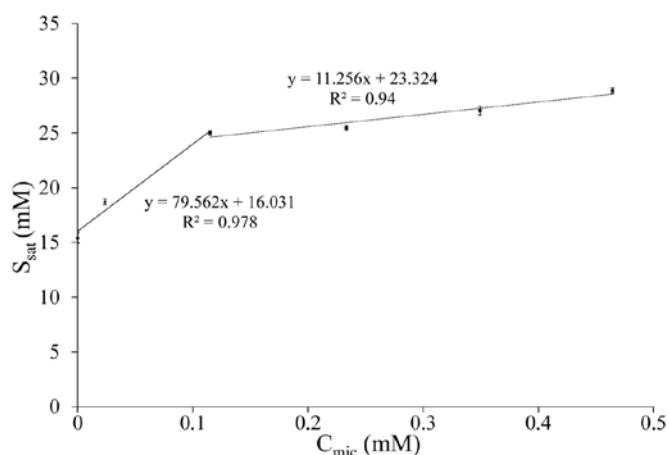


Figure 2. Plot of TMZ molar solubility in the pH 5.0 buffer (S_{sat}) at 25°C as a function of molar micellar concentration of F-PEG-HMD (C_{mic}). Each plot represents the observed mean $S_{\text{sat}} \pm \text{SD}$ (3 measures, $n=1$). Two regression lines were drawn, the correspondent equation and correlation coefficients (R^2) are indicated next to them.

Production of dry powders. The dry powders were produced by spray-drying F-PEG-HMD/TMZ nanomicelle solutions. Nanomicelle solutions were first prepared by co-solubilization of 1, 3, 5 and 9 mg/ml F-PEG-HMD and the highest possible amount of soluble TMZ in phosphate buffer at pH 5.0 (Table I). In order to evaluate the influence of the presence of TMZ on the physicochemical properties of the nanomicelle solutions, two TMZ-free nanomicelle solutions were prepared: Empty NS-1 and Empty NS-9 were prepared using 1 and 9 mg/ml F-PEG-HMD, respectively. The composition and physicochemical properties of Empty NS-1, Empty NS-9, NS-1, NS-3, NS-5 and NS-9 are presented in Table I. All the prepared nanomicelle solutions were characterized in a buffer at pH 5.0 by trimodal particle size distribution. Regarding the Z-average values, the size of the nanomicelles slightly increased with the concentrations of F-PEG-HMD and TMZ (Z-average of 50 ± 1 and 61 ± 3 nm for the NS-1 and NS-9 solutions, respectively). This increase in size seems to be attributed only to the increase in the F-PEG-HMD concentration (and not to the presence of TMZ), from the similar size increase from Empty NS-1 and Empty NS-9 (Z-average of 56.8 ± 0.8 and 68 ± 1 nm, respectively). However, the presence of TMZ seems to have a weak influence on the particle size distribution of the nanomicelles. The size and the PdI of the TMZ-loaded micellar solutions were a little lower than for the TMZ-free nanomicelle solutions, which characterizes a more homogeneous particle population. This could be explained by the fact that TMZ could participate in the structure of the nanomicelles, for example as a hydrophilic corona and/or by causing a reduction in the number of aggregations of the nanomicelles, leading to a more homogeneous particle size distribution and/or smaller size. Regarding the EE values in Table I, TMZ was difficult to entrap within the F-PEG-HMD nanomicelles: the EE observed were <10% in every nanomicelle solution. This could easily be explained by the physicochemical properties of TMZ. TMZ is a small molecule that, besides having low solubility in water (~3 mg/ml), cannot be considered as a lipophilic compound ($\log P \approx -1$). Consequently, its encapsulation within a hydrophobic core such as that composed by stearate chains

in the present nanomicelles represents a real challenge. The F-PEG-HMD concentration had no influence over the range of concentrations tested ($EE = \sim 9\%$) except for NS-1 (1 mg/ml F-PEG-HMD). For this, the EE observed was a little lower ($\sim 6\%$). The quite similar EE values observed from NS-3 to NS-9 also confirmed that TMZ does not induce an increase in size.

The NS-1, NS-3, NS-5 and NS-9 nanomicelle solutions were then spray-dried to produce dry powders. Spray-drying a buffer containing only F-PEG-HMD and TMZ led to poor yield ($\sim 40\%$) and to production of a sticky powder (data not shown). As mentioned above, stearate and PEG chains melt at a temperature $\sim 50^\circ\text{C}$, so spray-drying such low-melting compounds could lead to their partial melting. This issue was solved by adding hydrophilic carriers in solution, i.e. mannitol and leucine. Leucine has been widely employed as a component in DPI formulations for its ability to improve the dispersion properties of a dry powder (48-50). Different studies have shown that leucine allows the production of less cohesive particles due to its surfactant behavior (51). During the spray-drying process, leucine i) reduces the size of droplets, therefore ii) reduces the size of particles produced and iii) creates a coating around the dried particles (51). However, Kho and Hadinoto (52) observed that a single-carrier dry powder using leucine did not allow sufficient aqueous re-dispersibility of the initial nanomaterials. Leucine presents poor wettability properties that lead to poor re-dispersibility of nanomaterials (52). Therefore, mannitol was used in addition to leucine. Different proportions of F-PEG-HMD in the dry powders were tested, as presented in Table II. Production of all the dry powders led to yields between ~ 70 and $\sim 85\%$. After initial optimization, 20% w/w leucine (relative to total dried materials) was the most appropriate concentration in terms of aerosolization and flowability properties (data not shown).

The actual TMZ contents in Table II revealed that production of the SD-2.5 and SD-7.5 led to more similar TMZ contents than expected. Conversely, for the SD-12.5 and SD-22.5 formulations, which contained the highest proportions of F-PEG-HMD, the actual TMZ contents observed were much lower than the theoretical TMZ contents. An explanation would be that the SD-12.5 and SD-22.5 formulations probably do not have enough additional excipient (i.e. mannitol and leucine) to avoid large losses of F-PEG-HMD (and TMZ by extension, due to TMZ/F-PEG-HMD micellization) on the glass assembly of the spray-dryer. These losses are due to partial melting of PEG and/or stearate chains during the spray-drying process. However, very similar yields were obtained for all spray-dried formulations. Another preferred explanation would be that the loss of TMZ is due to preferential accumulation of the nanomicelles at the surface of the dried particles, which is a well-known problem with spray-dried nanocomposites (53). This problem is due to an expected high Péclet number [i.e. a dimensionless mass-transport number that compares the times for droplet drying and the dispersed/dissolved particle diffusion (53,54)] for the drying droplets, which results from the relative low diffusion coefficient of the nanomicelles compared to solubilized mannitol and leucine. As the process involves spray-drying a micellar solution composed of TMZ and F-PEG-HMD, TMZ is probably attracted by the nanomicelles to the surface of the dried

particles. As the surface of the dried materials contained higher proportions of TMZ/F-PEG-HMD in SD-12.5 and SD-22.5 than in SD-2.5 and SD-7.5, surface erosion during the spray-drying process led to much lower TMZ contents than expected.

The ability of the DPI formulations to release the F-PEG-HMD nanomicelles in aqueous media was evaluated. As described above, spray-drying involves high shear forces and an elevated temperature, which could induce irreversible aggregation of the spray-dried nanomicelles. In this case, dissolution of the DPI formulation in an aqueous media could lead to aggregated micelles with sizes $>1 \mu\text{m}$ or even lead to insoluble residues. Once dissolved in the buffer, none of the DPI formulations led to visible insoluble residues (no sediment formation, even after centrifugation), except for the SD-22.5 formulation. The nanomicelles resulting from the SD-2.5, SD-7.5 and SD-12.5 formulations were characterized by quite similar trimodal particle size distributions. These had maximum peaks at ~ 10 , ~ 75 and 470 nm , corresponding to relative intensities of ~ 5 , ~ 35 and $\sim 60\%$. The supernatant of the solution resulting from the SD-22.5 formulation presented larger nanomicelles than the three other DPI formulations (maximum peaks at ~ 25 , ~ 141 and 712 nm , corresponding to relative intensities of ~ 3 , ~ 50 and $\sim 43\%$). These results indicate that nanomicelles aggregate during spray drying for each DPI formulation. However, this aggregation was reduced and considered as acceptable in SD-2.5, SD-7.5 and SD-12.5. This was because it still led to the formation of nanomicelles and no insoluble residues were observed after reconstitution in the buffer.

Aerodynamic performance of the dry powders. The aerodynamic diameter is the most appropriate measure of aerosol particle size because it relates to particle dynamic behavior and describes the main mechanisms of aerosol deposition in the lung as both gravitational settling and inertial impaction (55). Aerosol particles need to present aerodynamic diameters of between 1 and $5 \mu\text{m}$ to reach the lower respiratory tract. By presenting optimal aerodynamic diameters, inhaled particles should be able to reach lung tumors to deliver their pharmacological effects and thus their therapeutic benefits.

In vitro pulmonary deposition and FPF values for the SD-2.5, SD-7.5, SD-12.5 and SD-22.5 formulations are presented in Fig. 3. SD-2.5 showed the best aerodynamic profile. It had the highest deposition in stages 3-5, corresponding to cut-off aerodynamic diameters $<5.27 \mu\text{m}$ at the flow rate of 100 l/min. Moreover, SD-2.5, and to lesser extent SD-7.5, led to a broad deposition, from the stages corresponding to the trachea to those illustrating the bronchioles and small terminal airways. In other words, SD-2.5 (and SD-7.5) might potentially be able to reach the lung tumor site(s) wherever it is located in the respiratory tract and might potentially lead to therapeutic benefits in lung cancer therapy. Conversely, SD-12.5 and especially SD-22.5 showed very poor aerodynamic properties, with a very low proportion of particles deposited in later stages (non-detectable values in stages 4 and 5; Fig. 3). They, therefore, cannot be considered as an inhalable dry powder. The *in vitro* pulmonary deposition profile revealed that SD-12.5 and SD-22.5 are mainly composed of large particles. More than 40-70%, respectively, of their particles were deposited

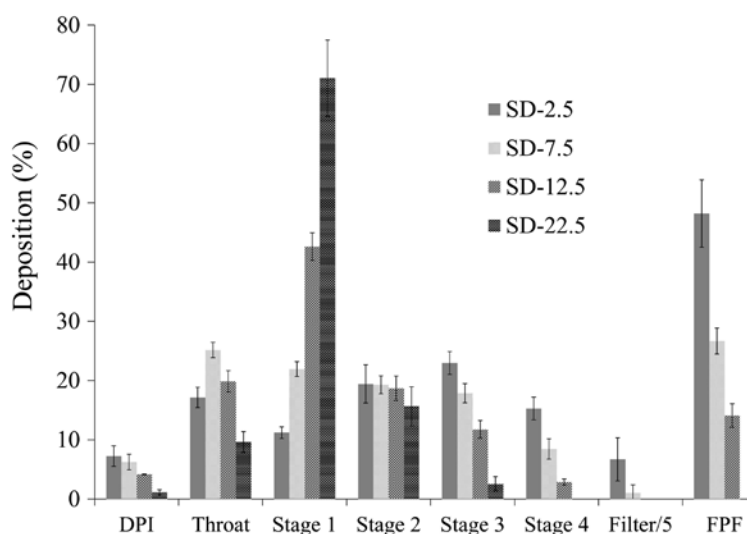


Figure 3. *In vitro* pulmonary deposition and fine particle fraction (FPF) values of the SD-2.5, SD-7.5, SD-12.5 and SD-22.5 formulations. Results are expressed as mean \pm SD (n=3).

in stage 1, which corresponds to the upper respiratory tract. Administration of one of these two formulations to a patient with a tumor located in the lower respiratory airway will lead inevitably to a treatment failure.

The proportion of F-PEG-HMD in the formulations had a direct influence on the aerodynamic properties of the dry powders: the smaller the proportion of F-PEG-HMD in the dry powders, the higher was the FPF (48 \pm 6 vs. 0% for SD-2.5 and SD-22.5, respectively). This could be explained by a partial melting of PEG and stearate chains in F-PEG-HMD (melting temperature, 50°C, see above) during spray drying (outlet temperature, 70°C), leading to large dried particles and large aerodynamic diameters (MMAD of 3.4 \pm 0.5, 4.4 \pm 0.4 and 5.82 \pm 0.08 μ m for SD-2.5, SD-7.5 and SD-12.5, respectively).

Regarding the *in vitro* lung deposition profiles obtained, it was concluded that SD-2.5 and SD-7.5 presented the best characteristics for potentially having a therapeutic efficacy against lung cancers located in the lower respiratory tract. This affirmation will be confirmed by future *in vivo* evaluations. Consequently, these two formulations were selected to pursue in the study.

***In vitro* release kinetics of TMZ.** The *in vitro* release kinetics of TMZ from formulations SD-2.5 and SD-7.5 were determined in simulated lung fluid (SLF) at 37°C and compared to the release from raw TMZ, which was used as a control. The release profiles are presented in Fig. 4.

The TMZ dissolution from raw TMZ, which is mainly dependent on the particle surface area [i.e. determined by the particle size distribution ($d(0.5) = 21.3 \pm 0.4 \mu\text{m}$)], was the fastest, with up to 77 and 90% dissolved within 20 and 30 min (significant different from formulations SD-2.5 and SD-7.5, $P < 0.05$, 1-way ANOVA test with Dunnett's multiple comparison test). Despite the higher particle surface area of TMZ particles in the dry powder (i.e. due to their smaller size and the hydrophilic matrix composed of the mannitol) the TMZ release from the dry powders seemed to be slightly lower. Moreover, the presence of F-PEG-HMD in the powder formulations seemed to have a slight effect on the TMZ release

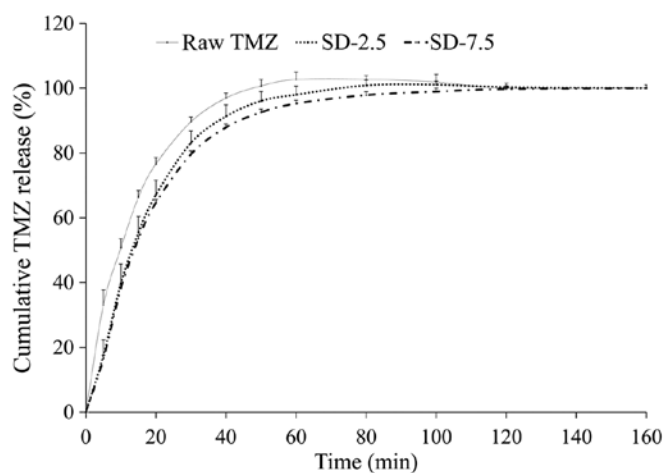


Figure 4. *In vitro* release kinetics of temozolomide from raw temozolomide, SD-2.5 and SD-7.5 formulations. Each point represents a mean observed TMZ concentration \pm SD (n=3).

in the SLF: the higher the proportion of F-PEG-HMD in the dry powder, the slower was the release (64 \pm 2, 67 \pm 4 and 77 \pm 2% released within 20 min for SD-2.5, SD7.5 and raw TMZ, respectively). These results tend therefore to prove interactions between TMZ and F-PEG-HMD in physiologic medium. These interactions induce a slowdown of the TMZ release from the formulations, as compared to raw TMZ. However, there is an indubitable similarity between the three curves [similarity factor $f_2(56) = 64$ and 59 for raw TMZ and SD-2.5 and for raw TMZ and SD-7.5, respectively]. The interactions between TMZ and F-PEG-HMD in physiological media seemed to be therefore limited. The similarity of the dissolutions profiles might be explained by the physicochemical properties of TMZ leading to two main issues for its sustained release from the dry powders. The first is that TMZ, while being a poorly water-soluble compound (solubility of ~ 3 mg/ml in water), cannot be considered as a lipophilic compound (logP-value of ~ 1). These physicochemical properties lead to the dry powders containing a high proportion of free TMZ (low *EE* values

Table III. Half maximal inhibitory concentration values (mM) of raw temozolomide and formulations SD-2.5 and SD-7.5 in one murine and one human lung cancer cell line.

Formulations	M109-HiFR lung carcinoma	A549 NSCLC
Raw TMZ	6.0±0.2	3.15±0.08
SD-2.5	5.9±0.1	3.3±0.1
SD-7.5	4.0±0.1	2.8±0.2

Results are expressed as mean ± SEM values (n=6).

in Table I). This is a high proportion of TMZ that does not interact with F-PEG-HMD nanomicelles, and that is therefore free to dissolve and release from the formulations in the same way as from raw TMZ. Secondly, TMZ is probably present in a very high proportion in the nanomicelle corona (rather than in the nanomicelle core), which is characterized by a relative higher hydrophilicity than the micelle core. The outside TMZ will be released in the medium very quickly, as compared to the share of TMZ included inside the nanomicelle core.

In vitro cytotoxic activity of the dry powders. The *in vitro* anti-proliferative properties of the dry powder formulations were evaluated by means of colorimetric MTT assay and compared to a solution of raw TMZ as a positive control. This viability assay is used to verify that TMZ conserves its *in vitro* anti-proliferative properties inside the dry powders.

All the IC₅₀ values of the tested TMZ-based DPI formulations (Table III) were similar to raw TMZ for the two cell lines tested. These results proved that TMZ is still active inside the DPI formulations *in vitro* and remains stable during all the formulation steps. As presumed, formulation SD-7.5 without TMZ (Empty SD-7.5) led to a >IC₅₀ compared to the highest concentration tested, which confirmed a good tolerance of the DPI formulations.

Discussion

DPI formulations composed of a new copolymer F-PEG-HMD were developed. The new copolymer F-PEG-HMD is able to self-assemble spontaneously in aqueous media as nanomicelles and can potentially interact with poorly water-soluble drugs, as is the case for most anticancer drugs. F-PEG-HMD is constituted of three main parts (Fig. 1): the loading compound, i.e. HMD, which should potentially be able to interact non-covalently with the drug; the targeting agent, i.e. the folate group; and the spacer, i.e. PEG, which should allow optimal interaction of the folate group and FR (to evaluate in future work). F-PEG-HMD nanomicelles should be at least as stable as most of the lipopolymer conjugates already described (24-26,46), considering its relatively low CMC value. High stability of the micelles after *in vivo* administration resulting from, among other characteristics, the CMC value is an important point to consider in order to guarantee their integrity (24,25). It is believed that the low volumes of lung fluids present in the respiratory tract [10-20 ml/100 m² (57)] and the low CMC obtained for F-PEG-HMD should guarantee the

micellar assembly of F-PEG-HMD after its administration as a dry powder by inhalation.

Although the physicochemical properties of TMZ make its encapsulation into nanovectors difficult (58), TMZ was chosen as cytotoxic drug model for this study due to its interesting anti-cancer properties in poor prognosis cancers such as glioblastoma and melanoma, as well as for lung cancer (31). We observed a non-negligible increase in TMZ solubility in water in the presence of F-PEG-HMD (2-fold increase of molar solubility in water). This increase in solubility could potentially lead to increased local concentrations in the tumor site after administration as a DPI. However, attention must be paid concerning the entrapment of TMZ within the F-PEG-HMD nanomicelles. A high proportion of TMZ contained in the dry powders is free to dissolve immediately in the medium. This 'free TMZ' proportion corresponds to i) non-entrapped TMZ and ii) adsorbed TMZ on the corona of the nanomicelles. Indeed, as previously described, TMZ is characterized as amphiphilic by nature and so TMZ should locate preferentially in the corona of nanomicelles. However, despite the probably low proportion of TMZ inside the core of the nanomicelles, we observed small differences in the release of TMZ from raw TMZ and dry powder formulations (Fig. 4). The main dissolution-limiting factor of raw TMZ is the particle surface area, determined by the particle size distribution (d(0.5)=21.3±0.4 μm). However, the main dissolution-limiting factors of TMZ from dry powder are: i) the particle surface area of the particles presenting a 'free TMZ' proportion on their surface, ii) the re-dispersibility of the nanomicelles from the dry powder and iii) the diffusion rate of TMZ from the nanomicelle corona (i.e. depending on the interactions between TMZ and F-PEG-HMD). The particle surface area of particles presenting a 'free TMZ' proportion on their surface in the dry powder should be higher (i.e. than raw TMZ particles) due to their smaller size. Moreover, the hydrophilic matrix composed of the mannitol and leucine allows a quick re-dispersibility of the nanomicelles, causing a considerable increase in the surface area (see aqueous re-dispersibility of the nanomicelles). Despite these two factors tending to increase the TMZ release from the dry powders, the TMZ release from the dry powders seems to be slightly lower. This is certainly due to the share of TMZ entrapped in the nanomicelle corona. TMZ is present in the powders with F-PEG-HMD, which should potentially be able to recognize the overexpressed FRs on the targeted lung tumor cells due to the grafted folate groups on the PEG extremities. Thus, once inhaled and deposited in the lung as shown *in vitro* by the acceptable FPF of the DPI formulations, the additional hydrophilic excipients, i.e. mannitol and leucine, dissolve quickly and rapidly release nanomicelles from the dry powders. This is shown *in vitro* by the recovery of the nanomicelles from the DPI formulations in water. This quick recovery therefore might permit the interaction between the folate groups and the FRs.

Another issue encountered with TMZ is the difficulty of evaluating its cytotoxic activity *in vitro*. TMZ is characterized by weak *in vitro* cytotoxic activity compared to other anticancer drugs, such as cisplatin (59). An *in vitro* evaluation of its anticancer activity is therefore in no way representative of the potent *in vivo* activity of TMZ against lung cancers. As an example, Mathieu *et al* (59) observed that TMZ had no

significant *in vitro* inhibitory effect on different melanoma cell lines (such as the mice B16F10 melanoma) at concentrations up to 10 μ M, although it displayed interesting *in vivo* activity on B16F10 mouse melanomas. As expected, IC₅₀ values in Table III confirmed the quite high IC₅₀ values (in the millimolar range), as reported in the literature (59,60).

The present study showed that it is possible to formulate dry powder for inhalation composed of a new self-assembling copolymer, F-PEG-HMD, and a cytotoxic drug, in this case TMZ. The developed DPI formulations are characterized by good aerodynamic properties and are able to release the nanomicelles quickly in aqueous media. This is especially true for the SD-2.5 and SD-7.5 formulations, which are characterized by FPFs of up to 50%. These two DPI formulations showed broad deposition in the impinger and should lead to a broad deposition in the lower respiratory tract, where adenocarcinomas are most frequently found. Assuming that F-PEG-HMD nanomicelles should recognize the lung adenocarcinoma cells through the overexpressed FRs (to be evaluated in future work), we can therefore conclude that F-PEG-HMD-based dry powders for inhalation could be an interesting drug delivery system that is able to release nanomicelles useful against adenocarcinomas that overexpress FRs. Future studies will evaluate our new F-PEG-HMD-based dry powder formulations. These formulations will be loaded with other anticancer drugs characterized by a higher lipophilicity than TMZ to allow drug encapsulation inside the core of the F-PEG-HMD nanomicelles.

Acknowledgements

Rémi Rosière was supported by a grant from the FRIA-FNRS (Fonds National de la Recherche Scientifique, Belgium). The analytical platform is supported by grants from the FRS-FNRS (Fonds de la Recherche Scientifique), no. 34553.08, and a grant from the FER 2007 (Fonds d'Encouragement à la Recherche, ULB).

References

1. Siegel RL, Miller KD and Jemal A: Cancer statistics, 2015. *CA Cancer J Clin* 65: 5-29, 2015.
2. Travis WD, Brambilla E, Noguchi M, Nicholson AG, Geisinger K, Yatabe Y, Powell CA, Beer D, Riely G, Garg K, *et al*: American Thoracic Society: International Association for the Study of Lung Cancer/American Thoracic Society/European Respiratory Society: international multidisciplinary classification of lung adenocarcinoma: executive summary. *Proc Am Thorac Soc* 8: 381-385, 2011.
3. Detterbeck FC, Boffa DJ and Tanoue LT: The new lung cancer staging system. *Chest* 136: 260-271, 2009.
4. Reck M, Heigener DF, Mok T, Soria JC and Rabe KF: Management of non-small-cell lung cancer: Recent developments. *Lancet* 382: 709-719, 2013.
5. O'Shannessy DJ, Yu G, Smale R, Fu YS, Singhal S, Thiel RP, Somers EB and Vachani A: Folate receptor alpha expression in lung cancer: Diagnostic and prognostic significance. *Oncotarget* 3: 414-425, 2012.
6. Cagle PT, Zhai QJ, Murphy L and Low PS: Folate receptor in adenocarcinoma and squamous cell carcinoma of the lung: Potential target for folate-linked therapeutic agents. *Arch Pathol Lab Med* 137: 241-244, 2013.
7. Christoph DC, Reyna-Asuncion B, Hassan B, Tran C, Maltzman JD, O'Shannessy DJ, Gauler TC, Wohlschlaeger J, Schuler M, Eberhardt WE, *et al*: Assessment of folate receptor- α and epidermal growth factor receptor expression in pemetrexed-treated non-small-cell lung cancer patients. *Clin Lung Cancer* 15: 320-30.e1, 3, 2014.
8. Bremer RE, Scoggin TS, Somers EB, O'Shannessy DJ and Tacha DE: Interobserver agreement and assay reproducibility of folate receptor α expression in lung adenocarcinoma: a prognostic marker and potential therapeutic target. *Arch Pathol Lab Med* 137: 1747-1752, 2013.
9. Gagnadoux F, Hureauux J, Vecellio L, Urban T, Le Pape A, Valo I, Montharu J, Leblond V, Boisdron-Celle M, Lerondel S, *et al*: Aerosolized chemotherapy. *J Aerosol Med Pulm Drug Deliv* 21: 61-70, 2008.
10. Wauthoz N, Deleuze P, Saumet A, Duret C, Kiss R and Amighi K: Temozolomide-based dry powder formulations for lung tumor-related inhalation treatment. *Pharm Res* 28: 762-775, 2011.
11. El-Gendy N and Berkland C: Combination chemotherapeutic dry powder aerosols via controlled nanoparticle agglomeration. *Pharm Res* 26: 1752-1763, 2009.
12. Alipour S, Montaseri H and Tafaghodi M: Preparation and characterization of biodegradable paclitaxel loaded alginate microparticles for pulmonary delivery. *Colloids Surf B Biointerfaces* 81: 521-529, 2010.
13. Meenach SA, Anderson KW, Zach Hilt J, McGarry RC and Mansour HM: Characterization and aerosol dispersion performance of advanced spray-dried chemotherapeutic PEGylated phospholipid particles for dry powder inhalation delivery in lung cancer. *Eur J Pharm Sci* 49: 699-711, 2013.
14. Sanna V, Pala N and Sechi M: Targeted therapy using nanotechnology: Focus on cancer. *Int J Nanomed* 9: 467-483, 2014.
15. Xu X, Ho W, Zhang X, Bertrand N and Farokhzad O: Cancer nanomedicine: From targeted delivery to combination therapy. *Trends Mol Med* 21: 223-232, 2015.
16. Mansour HM, Rhee YS and Wu X: Nanomedicine in pulmonary delivery. *Int J Nanomed* 4: 299-319, 2009.
17. Kumar A, Dailey LA and Forbes B: Lost in translation: What is stopping inhaled nanomedicines from realizing their potential? *Ther Deliv* 5: 757-761, 2014.
18. Sung JC, Pulliam BL and Edwards DA: Nanoparticles for drug delivery to the lungs. *Trends Biotechnol* 25: 563-570, 2007.
19. Verschraegen CF, Gilbert BE, Loyer E, Huaranga A, Walsh G, Newman RA and Knight V: Clinical evaluation of the delivery and safety of aerosolized liposomal 9-nitro-20(s)-camptothecin in patients with advanced pulmonary malignancies. *Clin Cancer Res* 10: 2319-2326, 2004.
20. Densmore CL, Kleinerman ES, Gautam A, Jia SF, Xu B, Worth LL, Waldrep JC, Fung YK, T'Ang A and Knight V: Growth suppression of established human osteosarcoma lung metastases in mice by aerosol gene therapy with PEI-p53 complexes. *Cancer Gene Ther* 8: 619-627, 2001.
21. Gautam A, Waldrep JC, Kleinerman ES, Xu B, Fung YK, T'Ang A and Densmore CL: Aerosol gene therapy for metastatic lung cancer using PEI-p53 complexes. *Methods Mol Med* 75: 607-618, 2003.
22. Khanna C, Anderson PM, Hasz DE, Katsanis E, Neville M and Klausner JS: Interleukin-2 liposome inhalation therapy is safe and effective for dogs with spontaneous pulmonary metastases. *Cancer* 79: 1409-1421, 1997.
23. Vadakkan MV, Annapoorna K, Sivakumar KC, Mundayoor S and Kumar GSV: Dry powder cationic lipopolymeric nanomicelle inhalation for targeted delivery of antitubercular drug to alveolar macrophage. *Int J Nanomed* 8: 2871-2885, 2013.
24. Lukyanov AN and Torchilin VP: Micelles from lipid derivatives of water-soluble polymers as delivery systems for poorly soluble drugs. *Adv Drug Deliv Rev* 56: 1273-1289, 2004.
25. Torchilin VP: Micellar nanocarriers: Pharmaceutical perspectives. *Pharm Res* 24: 1-16, 2007.
26. Torchilin VP: Structure and design of polymeric surfactant-based drug delivery systems. *J Control Release* 73: 137-172, 2001.
27. Wauthoz N, Deleuze P, Hecq J, Roland I, Saussez S, Adanja I, Debeir O, Decaestecker C, Mathieu V, Kiss R, *et al*: In vivo assessment of temozolomide local delivery for lung cancer inhalation therapy. *Eur J Pharm Sci* 39: 402-411, 2010.
28. Newlands ES, Stevens MFG, Wedge SR, Wheelhouse RT and Brock C: Temozolomide: A review of its discovery, chemical properties, pre-clinical development and clinical trials. *Cancer Treat Rev* 23: 35-61, 1997.
29. Kanzawa T, Germano IM, Komata T, Ito H, Kondo Y and Kondo S: Role of autophagy in temozolomide-induced cytotoxicity for malignant glioma cells. *Cell Death Differ* 11: 448-457, 2004.
30. Roos WP, Batista LFZ, Naumann SC, Wick W, Weller M, Menck CFM and Kaina B: Apoptosis in malignant glioma cells triggered by the temozolomide-induced DNA lesion O⁶-methylguanine. *Oncogene* 26: 186-197, 2007.

31. Lefranc F, Facchini V and Kiss R: Proautophagic drugs: A novel means to combat apoptosis-resistant cancers, with a special emphasis on glioblastomas. *Oncologist* 12: 1395-1403, 2007.
32. Pietanza MC, Kadota K, Huberman K, Sima CS, Fiore JJ, Sumner DK, Travis WD, Heguy A, Ginsberg MS, Holodny AI, *et al*: Phase II trial of temozolomide in patients with relapsed sensitive or refractory small cell lung cancer, with assessment of methylguanine-DNA methyltransferase as a potential biomarker. *Clin Cancer Res* 18: 1138-1145, 2012.
33. Kouroussis C, Vamvakas L, Vardakis N, Kotsakis A, Kalykaki A, Kalbakis K, Saridaki Z, Kentepozidis N, Giassas S and Georgoulis V: Continuous administration of daily low-dose temozolomide in pretreated patients with advanced non-small cell lung cancer: A phase II study. *Oncology* 76: 112-117, 2009.
34. Adonizio CS, Babb JS, Maiale C, Huang C, Donahue J, Millenson MM, Hosford M, Somer R, Treat J, Sherman E, *et al*: Temozolomide in non-small-cell lung cancer: Preliminary results of a phase II trial in previously treated patients. *Clin Lung Cancer* 3: 254-258, 2002.
35. Choong NW, Mauer AM, Hoffman PC, Rudin CM, Winegarden JD III, Villano JL, Kozloff M, Wade JL III, Sciortino DF, Szeto L, *et al*: Phase II trial of temozolomide and irinotecan as second-line treatment for advanced non-small cell lung cancer. *J Thorac Oncol* 1: 245-251, 2006.
36. Trinh VA, Patel SP and Hwu WJ: The safety of temozolomide in the treatment of malignancies. *Expert Opin Drug Saf* 8: 493-499, 2009.
37. Maldonado F, Limper AH, Lim KG and Aubrey MC: Temozolomide-associated organizing pneumonitis. *Mayo Clin Proc* 82: 771-773, 2007.
38. Aronov O, Horowitz AT, Gabizon A and Gibson D: Folate-targeted PEG as a potential carrier for carboplatin analogs. Synthesis and in vitro studies. *Bioconjug Chem* 14: 563-574, 2003.
39. Dhar S, Liu Z, Thomale J, Dai H and Lippard SJ: Targeted single-wall carbon nanotube-mediated Pt(IV) prodrug delivery using folate as a homing device. *J Am Chem Soc* 130: 11467-11476, 2008.
40. Alvarez-Núñez FA and Yalkowsky SH: Relationship between polysorbate 80 solubilization descriptors and octanol-water partition coefficients of drugs. *Int J Pharm* 200: 217-222, 2000.
41. Marques MRC, Loebenberg R and Almkainzi M: Simulated biological fluids with possible application in dissolution testing. *Dissolution Technol* 18: 15-28, 2011.
42. Gill KK, Nazzal S and Kaddoumi A: Paclitaxel loaded PEG(5000)-DSPE micelles as pulmonary delivery platform: Formulation characterization, tissue distribution, plasma pharmacokinetics, and toxicological evaluation. *Eur J Pharm Biopharm* 79: 276-284, 2011.
43. Gabizon A, Horowitz AT, Goren D, Tzemach D, Mandelbaum-Shavit F, Qazen MM and Zalipsky S: Targeting folate receptor with folate linked to extremities of poly(ethylene glycol)-grafted liposomes: In vitro studies. *Bioconjug Chem* 10: 289-298, 1999.
44. Chen H, Zhang T, Zhou Z, Guan M, Wang J, Liu L and Zhang Q: Enhanced uptake and cytotoxicity of folate-conjugated mitoxantrone-loaded micelles via receptor up-regulation by dexamethasone. *Int J Pharm* 448: 142-149, 2013.
45. Berger G, Gasper R, Lamoral-Theys D, Wellner A, Gelbecke M, Gust R, Nève J, Kiss R, Goormaghtigh E and Dufresne F: Fourier transform infrared (FTIR) spectroscopy to monitor the cellular impact of newly synthesized platinum derivatives. *Int J Oncol* 37: 679-686, 2010.
46. Ke X, Ng VWL, Ono RJ, Chan JM, Krishnamurthy S, Wang Y, Hedrick JL and Yang YY: Role of non-covalent and covalent interactions in cargo loading capacity and stability of polymeric micelles. *J Control Release* 193: 9-26, 2014.
47. Icoz DZ, Moraru CI and Kokini JL: Polymer-polymer interactions in dextran systems using thermal analysis. *Carbohydr Polym* 62: 120-129, 2005.
48. Rabbani NR and Seville PC: The influence of formulation components on the aerosolisation properties of spray-dried powders. *J Control Release* 110: 130-140, 2005.
49. Seville PC, Learoyd TP, Li HY, Williamson IJ and Birchall JC: Amino acid-modified spray-dried powders with enhanced aerosolisation properties for pulmonary drug delivery. *Powder Technol* 178: 40-50, 2007.
50. Sou T, Kaminskas LM, Nguyen TH, Carlberg R, McIntosh MP and Morton DAV: The effect of amino acid excipients on morphology and solid-state properties of multi-component spray-dried formulations for pulmonary delivery of biomacromolecules. *Eur J Pharm Biopharm* 83: 234-243, 2013.
51. Pilcer G and Amighi K: Formulation strategy and use of excipients in pulmonary drug delivery. *Int J Pharm* 392: 1-19, 2010.
52. Kho K and Hadinoto K: Effects of excipient formulation on the morphology and aqueous re-dispersibility of dry-powder silica nano-aggregates. *Colloids Surfaces A Physicochem Eng Asp* 359: 71-81, 2010.
53. Duret C, Wauthoz N, Sebti T, Vanderbist F and Amighi K: New inhalation-optimized itraconazole nanoparticle-based dry powders for the treatment of invasive pulmonary aspergillosis. *Int J Nanomed* 7: 5475-5489, 2012.
54. Stroock AD, Dertinger SKW, Ajdari A, Mezić I, Stone HA and Whitesides GM: Chaotic mixer for microchannels. *Science* 295: 647-651, 2002.
55. Pilcer G, Wauthoz N and Amighi K: Lactose characteristics and the generation of the aerosol. *Adv Drug Deliv Rev* 64: 233-256, 2012.
56. Shah VP, Tsong Y, Sathe P and Liu JP: In vitro dissolution profile comparison - statistics and analysis of the similarity factor, f2. *Pharm Res* 15: 889-896, 1998.
57. Patton JS: Mechanisms of macromolecule absorption by the lungs. *Adv Drug Deliv Rev* 19: 3-36, 1996.
58. Tian XH, Lin XN, Wei F, Feng W, Huang ZC, Wang P, Ren L and Diao Y: Enhanced brain targeting of temozolomide in polysorbate-80 coated polybutylcyanoacrylate nanoparticles. *Int J Nanomed* 6: 445-452, 2011.
59. Mathieu V, Le Mercier M, De Neve N, Sauvage S, Gras T, Roland I, Lefranc F and Kiss R: Galectin-1 knockdown increases sensitivity to temozolomide in a B16F10 mouse metastatic melanoma model. *J Invest Dermatol* 127: 2399-2410, 2007.
60. Appel EA, Rowland MJ, Loh XJ, Heywood RM, Watts C and Scherman OA: Enhanced stability and activity of temozolomide in primary glioblastoma multiforme cells with cucurbit[n]uril. *Chem Commun (Camb)* 48: 9843-9845, 2012.